

Preparation, characterization and photocatalytic degradation of Congo Red by ZnZrO₃/ZnO/ZrO₂

Azadeh Moradzadeh¹, Alireza Mahjoub^{2,*}, Mir Abdullah Seyd Sadjadi^{1,*},
Moayad Hossaini Sadr³ and Nazanin Farhadyar⁴

¹Department of Chemistry, Science and Research Branch, Islamic Azad University, Tehran, Iran

²Department of Chemistry, Tarbiat Modares University, Box 14115-111, Jalal Aleahmad, Tehran, Iran

³Department of Chemistry, Azarbaijan Shahid Madani University, Tabriz, Iran

⁴Department of Chemistry, Islamic Azad University, Varamin-Pishva, Iran

Received 13 May 2019;

revised 23 August 2019;

accepted 26 August 2019;

available online 29 August 2019

Abstract

Un-doped and Cd-doped ZnZrO₃/ZnO/ZrO₂ nano composites (CDZZ-NCPs) (CD0-4) were synthesized by the hydrothermal method. The nano composites were characterized by various techniques such as Fourier Transform Infra-Red spectroscopy (FT-IR), X-ray Diffraction (XRD), Field Emission Scanning Electron Microscopy (FE-SEM) and Energy Dispersive X-Ray Analysis (EDS). The photocatalytic properties of CDZZ-NCPs (CD0-4) were studied by degradation of congo red (CR) dye under sunlight irradiation. The results reveal unique sunlight photocatalytic ability for the degradation of CR. The experimental demonstrated that the 0.03 g of ZnZrO₃/ZnO/ZrO₂ nano composites can degrade 50 mL of CR solution (10 ppm) during 5 minutes (up to 91.3%).

Keywords: Congo Red; Nanocomposite Catalyst; Photocatalysis; Photocatalytic Degradation; Zirconium dioxide; Zinc Oxide; Zinc Zirconate.

How to cite this article

Moradzadeh A, Mahjoub A, Seyd Sadjadi MA, Sadr MH, Farhadyar N. Preparation, characterization and photocatalytic degradation of Congo Red by ZnZrO₃/ZnO/ZrO₂. Int. J. Nano Dimens., 2020; 11 (1): 32-40.

INTRODUCTION

The development of dye industries leads to increasing environmental pollutions such as soil, surface water and underground water contamination. Azo dyes from the textile industry are a major water pollution source. Congo red (CR) C₃₂H₂₂N₆Na₂O₆S₂ is a toxic azo dye used in the textile industry that can affect the human body [1], plants and the ecosystem of organisms living in the water. Therefore, water purification is one of the most vital requirements for the conservation of water resources for the development of the world. To overcome congo red degradation from sewage, semiconductors as a catalyst has recently attached extensive attention.

Perovskites (ABO₃ (A²⁺B⁴⁺X²⁻)) has attached attention due good photocatalytic activity and well efficiency for degradation of azo dyes [2-5]. Perovskites can be classified as follows: (a)

Titanate, (b) Zirconate, (c) Tantalate, (d) Niobium Based, (e) Vanadium Based, (f) Ferrite Based, (g) Bismuth Based, (h) Cobalt Based, (i) Nickel Based, (j) Chromium Based, (k) Double Perovskites (A₂B₂O₆) and Other Perovskites Systems [6]. The zinc zirconate (ZnZrO₃) (ZZ), zinc oxide (ZnO) (ZO) and zirconium oxide (ZrO₂) (ZRO) nanoparticles are studied by Habibi [7]. Nanoporous ZZ, ZO and ZRO thin films were prepared by sol-gel method for improving the fill factor (ff) of the dye sensitized solar cells. In another study, Zhu [8] were synthesized and studied Optical properties of perovskite ZnZrO₃ nanoparticles.

Zinc oxide has been long studied to degradation and decolorization of congo red dye [9, 10]. ZnO can absorb UV light (less than 387 nm) due to large band gap (3.37). Therefore, ZnO doping with metal or non-metals [11] can improve its photocatalytic activity in the visible light region. Wu [12] prepared ZnO

* Corresponding Author Email: mahjouba@modares.ac.ir

by the sol-gel method. The results of their research revealed that methyl orange was removed (99.70 %) under UV irradiation. Photocatalytic degradation of congo red using zinc oxide was investigated by Jacob White [13]. The results indicate that rate of degradation is dependent on temperature. A kinetic study on the adsorption of congo red from aqueous solution by ZnO-ZnFe₂O₄ nanocomposite was studied by Karamipour [14]. Exploration of various nano ZnO catalysts was studied by Preethi [15] to degradation of congo red dye. They prepared nano zinc oxide by three methods (precipitation, pyrolytic and combustion). The results indicated good degradation efficiency for congo red.

Nanocomposites contain ZrO₂ exhibit degradation or adsorption of congo red dye [16, 17]. Photocatalytic property of nano ZrO₂-SnO₂ NPs for degradation of congo red was studied by Aghabeygi [18]. The result shows high efficiency of degradation of congo red under UV irradiation (96% after 30 min). Wang [19] fabricated porous ZrO₂ hollow sphere and its adsorption performance to congo red in the water. Degradation of congo red dye by a Fe₂O₃-CeO₂-ZrO₂/palygorskite composite catalyst was studied by Ouyang [20] and the result indicated that the adsorption efficiency of CR was up to 95%.

In this work, Cd-doped ZnZrO₃/ZnO/ZrO₂ nano composites (CDZZ-NCPs) were prepared by the

hydrothermal method for the degradation of CR dye. Among the perovskites, photocatalytic study of zinc zirconate is rare. The purpose of this research is to investigate the degradation of CR dye by un-doped and Cd-doped ZnZrO₃/ZnO/ZrO₂ nano composites (CDZZ-NCPs) under sunlight for the first time. Degradation photocatalytic process showed high decomposition of congo-red dye in a short time (91.3% - 5 min).

EXPERIMENTAL

Starting materials

Un-doped and Cd-doped ZnZrO₃/ZnO/ZrO₂ nano composites (CDZZ-NCPs) were synthesized by hydrothermal method. Zinc acetate dehydrate [Zn(CH₃COO)₂. 2H₂O] 99.5%-Merck, cadmium acetate dihydrate [Cd(CH₃COO)₂. 2H₂O] 99.2 %-Merck, and zirconium (IV) isopropoxide [Zr(IPP)] solution 70 wt% in propanol Zr[OCH₂CH₂CH₃]₄; Sigma-Aldrich were starting materials for Zn, Cd and Zr, respectively. Congo red (CR) C₃₂H₂₂N₆Na₂O₆S₂-Merck was used to study photocatalytic activity.

Synthesis of catalysis

The preparation steps of ZnZrO₃/ZnO/ZrO₂ nanocomposite (CDZZ-NCPs) are shown in Fig. 1. Firstly, various amounts of Zn(Ac)₂ and Cd(Ac)₂ (Table 1) were dissolved into 10 mL ethanol (30 min) to obtain a transparent solution, then

Table 1. Various amounts used to prepare un-doped and Cd doped ZnZrO₃/ZnO/ZrO₂ nano composites (CDZZ-NCPs) (CD0-4).

Product	Symbol	Zn(Ac) ₂ . 2H ₂ O (g)	Cd(Ac) ₂ . 2H ₂ O (g)	Zr (IPP) (mL)
Un-doped ZZ-NCPs	CD0	2.66	-	1.344
CDZZ-NCPs	CD1	2.527	0.16	1.344
CDZZ-NCPs	CD2	2.39	0.32	1.344
CDZZ-NCPs	CD3	2.26	0.48	1.344
CDZZ-NCPs	CD4	2.12	0.64	1.344

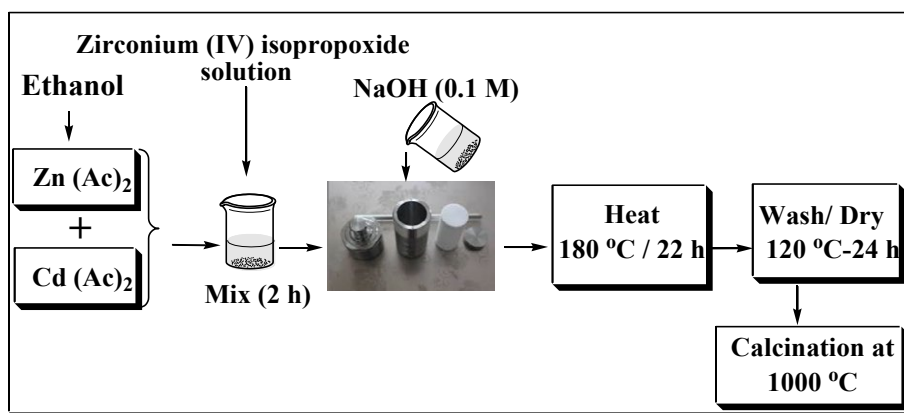


Fig. 1. The preparation steps of ZnZrO₃/ZnO/ZrO₂ nano composites (CDZZ-NCPs) (CD0-4).

the zirconium isopropoxide were added to the solution and mixed under magnetic stirring for about 2h at room temperature. We labeled (CD0) for un-doped $ZnZrO_3/ZnO/ZrO_2$ and (CD1-4) for various amounts of Cd in the $ZnZrO_3/ZnO/ZrO_2$ nanocomposite (Table 1). The molar ratio of Zn+Cd/Zr was 4:1 and totally was fixed at 0.5 M. Teflon autoclave with a capacity of 70 cc filled by the final mixture (~80% fill). Sodium hydroxide (1.0 M) as mineralizer was added to the mixture [8]. The autoclave was sealed and heated at 180 °C for 22 h. The final products were filtered, washed with distilled water to remove extra ligands. It was dried for 24 h in oven at 120 °C and calcinated at 1000 °C for 8h in air.

Characterization of catalysts

The obtained powder were characterized by FT-IR (Thermo Nicolet, Nexus 870, America) to identifying various functional groups present in product, XRD (STOE, STADI P, Germany, Radiation: 1.54060 Cu Ka) to study the structure and crystalline phase of the obtained product, FE-SEM (MIRA3, TE-SCAN, Czech Republic) to provide general morphologies, EDS [MIRA3, TE-SCAN, SAMX detector (France), Czech Republic] to analyze the elemental composition of solid surfaces and UV-Vis spectrophotometer (Varian, Cary 100 Conc. Australia) to investigate the photocatalytic activity.

Photocatalytic experimental

The photocatalytic activity of CDZZ-NCPs (CD0-4) was evaluated using the degradation of CR under

sunlight irradiation. In a typical process, 0.03 g of nanocomposite was dispersed in 50 mL of CR aqueous solution (10 ppm), to reach adsorption-desorption equilibrium of CR on the CDZZ-NCPs (CD0-4) surface, the solution was kept in the dark for 30 min before it was exposed to sunlight. Then, the mixture was exposed to sunlight under the magnet stirring to evaluate the degradation of CR dye. Each 5 minutes 3 mL of the mixture was taken out, centrifuged and was recorded by a UV-Vis spectrophotometer at the maximum absorption wavelength of the CR (350-650 nm). Following equation: $\% \text{ Degradation} = (A_0 - A_t/A_0) \times 100$ was used to calculate CR degradation percentage, where A_0 and A_t are initial and the solution adsorption value after irradiation time (t), respectively.

RESULT AND DISCUSSION

FT-IR of CDZZ-NCPs (CD0-4)

Fig. 2. demonstrates the FT-IR spectra of the CDZZ-NCPs (CD0-4). The absorption bonds at about 782-656 cm^{-1} are assigned to the stretching vibration of (M-L) (M = Zn, Cd and Zr) bonds [21]. The broad absorption bonds at 501-564 cm^{-1} are ascribed to the stretching vibration of (M-O) (M = Zn, Cd and Zr) bonds, which is consistent with the XRD and EDS data and did not contain significant further absorption bond in the wavelength greater than 1000 cm^{-1} [22]. These results indicate the successful synthesis of CDZZ-NCPs (CD0-4) via a hydrothermal method followed by calcination. Table 2 shows the detailed assignments of the peaks for the five samples.

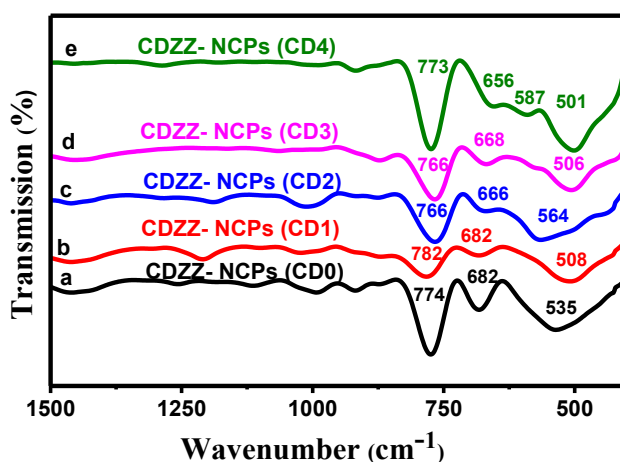


Fig. 2. FT-IR spectra of (a) un-doped $ZnZrO_3/ZnO/ZrO_2$ (CD0), (b) CDZZ-NCPs (CD1), (c) CDZZ-NCPs (CD2), (d) CDZZ-NCPs (CD3) and (e) CDZZ-NCPs (CD4).

Table 2. Assignments of the peaks in FT-IR spectra of CDZZ-NCPs (CD0-4).

Assignment	CD0	CD1	CD2	CD3	CD4
ν (M-O) bond	535 (cm ⁻¹)	508 (cm ⁻¹)	564 (cm ⁻¹)	506 (cm ⁻¹)	501 (cm ⁻¹) 587 (cm ⁻¹)
ν (M-L) bond	682 (cm ⁻¹) 774 (cm ⁻¹)	682 (cm ⁻¹) 782 (cm ⁻¹)	666 (cm ⁻¹) 766 (cm ⁻¹)	668 (cm ⁻¹) 766 (cm ⁻¹)	656 (cm ⁻¹) 773 (cm ⁻¹)

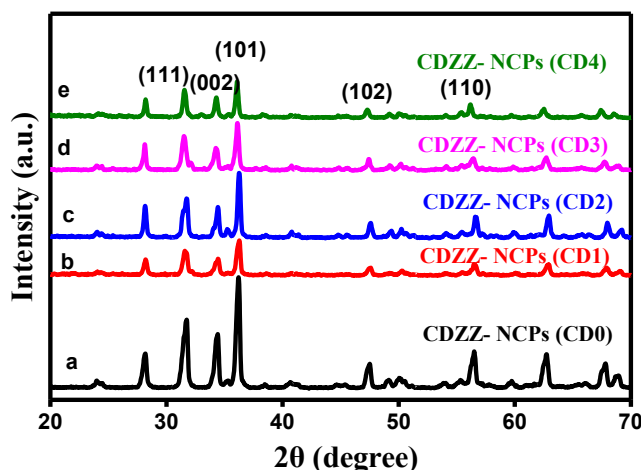


Fig. 3. XRD pattern of (a) ZZ-NCPs (CD0), (b) CDZZ-NCPs (CD1), (c) CDZZ-NCPs (CD2), (d) CDZZ-NCPs (CD3) and (e) CDZZ-NCPs (CD4).

Table 3. Average particle sizes (nm) and Atomic concentrations (at. %) of Zn: Cd: Zr: O of CDZZ-NCPs (CD0-4).

Symbol of nanocatalyst	average particle sizes (nm)	Zn w%	Cd w%	Zr w%	O w%
CD0	64	56.35	---	25.00	18.65
CD1	78	71.62	0.88	10.26	17.24
CD2	58	43.51	2.33	37.85	16.31
CD3	28	73.76	4.49	5.56	16.19
CD4	26	53.15	8.12	22.83	15.89

XRD of CDZZ-NCPs (CD0-4)

Fig. 3. illustrates comparing XRD pattern of un-doped ZnZrO₃/ZnO/ZrO₂ (CD0) [Fig. 3(a)] and Cd doped-ZnZrO₃/ZnO/ZrO₂ (CDZZ-NCPs) (CD1-4) [Fig. 3(b-e)], used to characterize the crystal phases and crystallinity. The crystalline reflection of the samples demonstrates three phases of ZnZrO₃ (JCPDS No 00-032-1482), Hexagonal phase of zinc oxide (JCPDS No 01-076-0704) and Monoclinic phase of zirconium dioxide (JCPDS No 01-083-0940).

The Scherrer equation was used in the determination of size of particles: Particle size = $(0.9 \times \lambda) / (d \cos\theta)$, where X-ray wavelength (λ) is 0.154 nm, d is the line broadening at half the maximum intensity (FWHM) and θ is the Bragg angle [23]. The average crystalline sizes calculated from the above equation for CD0-4 were 43.4 nm,

34.9 nm, 33.9 nm, 28.8 nm and 24.3 nm in order. The calculated crystalline size of the as synthesized photocatalysts shows that the crystalline size of CDZZ-NCPs (CD0-4) were decreased with the increase of Cd-dopant in the photocatalysts CDZZ-NCPs (CD2-4).

FE-SEM and EDS of CDZZ-NCPs (CD0-4)

The FE-SEM images of prepared CDZZ-NCPs (CD0-4) are shown in Fig. 4 (a-e) respectively. The FE-SEM images result indicates that the average particle sizes of the final composite decreases from approximately 64 nm for un-doped ZZ-NCPs (CD0) (Fig. 4a) to approximately 58 nm when Cd-dopant is added from CDZZ-NCPs (CD2) (Fig. 4c), and further down to approximately 28 nm and 26 nm for CDZZ-NCPs (CD3-4) in order (Fig. 4 (d-e)). The decrease in the average particle sizes happens with

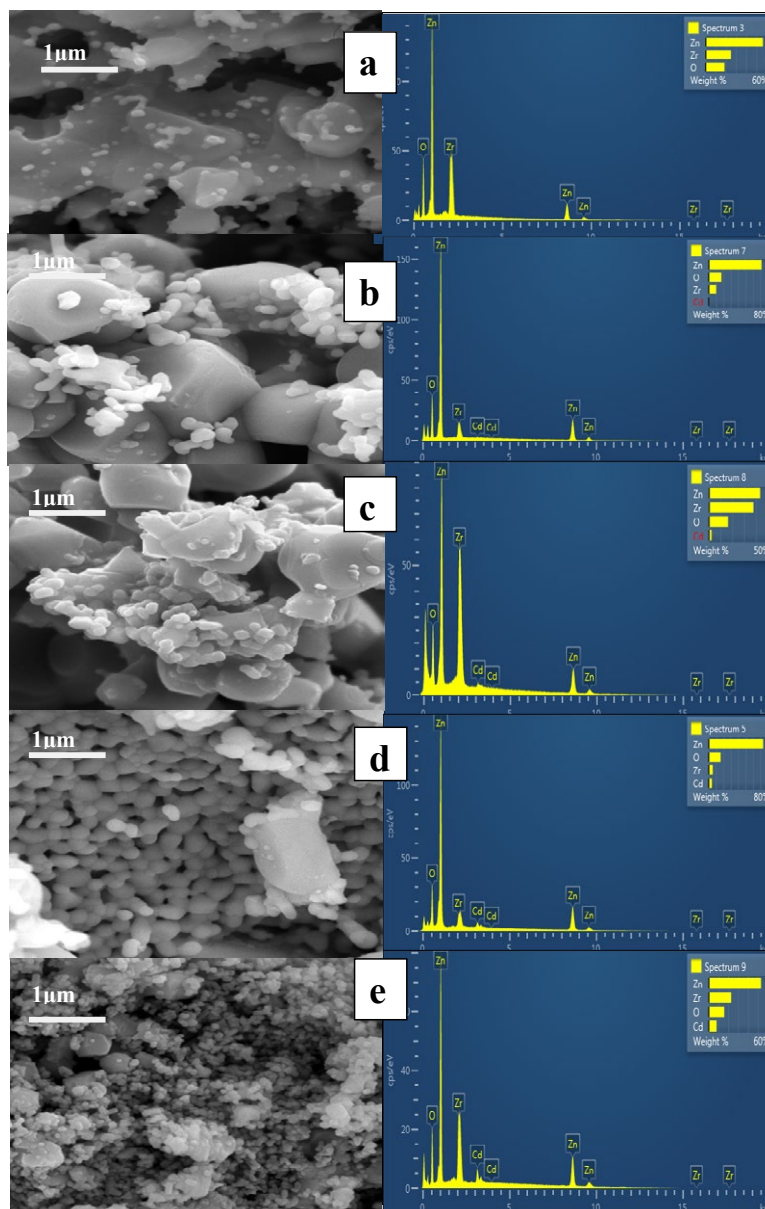


Fig. 4. FE-SEM pictures and EDS of (a) un-doped ZZ-NCPs (CD0), (b) CDZZ-NCPs (CD1), (c) CDZZ-NCPs (CD2), (d) CDZZ-NCPs (CD3) and (e) CDZZ-NCPs (CD4).

increasing of Cd-dopant from CDZZ-NCPs (CD0) to CDZZ-NCPs (CD1-4) (Table 3). To investigate the molar ratio of the elements present in the nanocomposite, characterization was done with the EDS. The atomic concentrations results are presented in the Table 3. Fig. 4 (a-e) illustrates the EDS spectrum of CDZZ-NCPs (CD0-4) respectively. The presence of Zinc, Cadmium, Zirconium and Oxygen peaks confirms the particles were made of Zn, Cd, Zr and O elements. Atomic concentrations (at. %) of Zn: Cd: Zr: O are: (CD0 = 56.35: 0.00:

25.00: 18.65), (CD1 = 71.62: 0.88: 10.26: 17.24), (CD2 = 43.51: 2.33: 37.85: 16.31), (CD3 = 73.76: 4.49: 5.56: 16.19) and (CD4 = 53.15: 8.12: 22.83: 15.89), which is taken from quantitative EDS analyses results.

PHOTOCATALYTIC PERFORMANCE OF CDZZ-NCPs (CD0-4)

Fig. 5. demonstrates removal rates results from the time dependent UV-Vis absorption spectra. Fig. 5 (a) shows UV-Vis absorption spectra of only

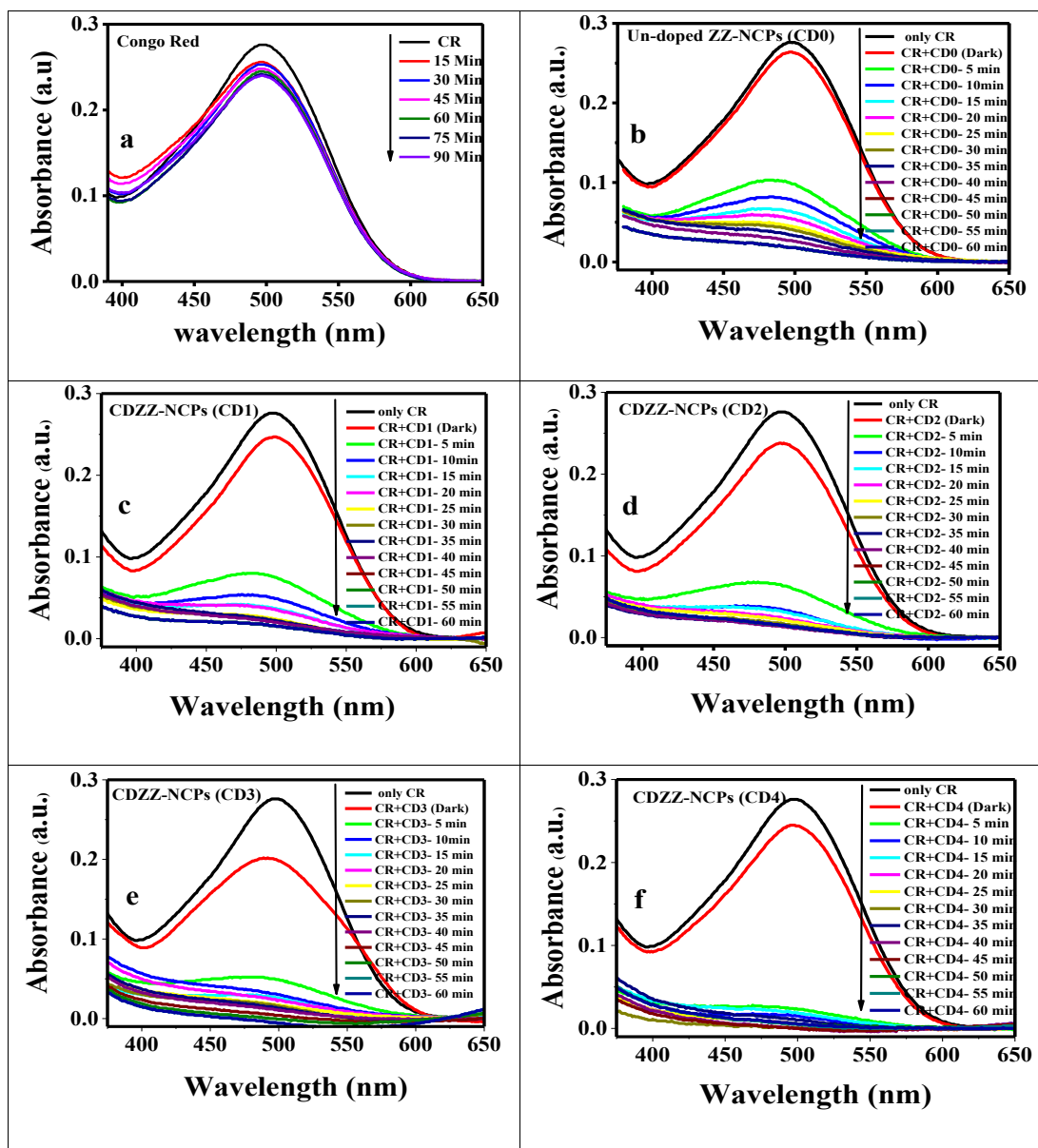


Fig. 5. UV-Vis Absorption spectra of (a) CR alone, (b) un-doped ZZ-NCPs (CD0) and (c-f) CDZZ-NCPs (CD1-4).

CR solution when exposed to sunlight and Fig. 5 (b-f) shows UV-Vis absorption spectra of CR solution mixed with un-doped and Cd doped of ZnZrO₃/ZnO/ZrO₂ [CDZZ-NCPs (CD0-4)] in pH =14, which were adjusted using NaOH. The congo red main absorption peak occurs at 498 nm and intensity decreases from 0.28 to 0.24 when only CR was exposed to sunlight irradiation for 90 minutes [Fig. 5 (a)]. In comparison, the degradation rate facilitated after adding 0.03 g catalyst [un-doped/ CDZZ-NCPs (CD0-4)] into the 50 mL of

CR solution (10 ppm) under sunlight [fig. 5 (b-f)]. The best degradation ratio of CR dye, occurs at alkaline pH (pH =14). Surface-charge properties of photocatalyst CDZZ-NCPs (CD0-4) and the natural properties of CR could be attributed this phenomenon. Congo red is an azo dye with two sulfonic groups, which can ionize and make a CR anion. The surface of nanocatalyst CDZZ-NCPs (CD0-4) in the high alkaline regions (pH=14) have a very high positive surface potential charge (Zeta-point charge = +17.6). Positive surface of

Table 4. Compare the degradation rate, (D %) of CDZZ-NCPs (CD0-4).

Catalysts	D% 5 min	D% 10 min	D% 15 min	D% 20 min	D% 25 min	D% 30 min	D% 45 min	D% 60 min
Un-doped ZZ-NCPs (CD0)	64.1 %	71.5 %	76.8 %	80.0 %	83.6 %	85.1 %	93.3 %	93.4 %
CDZZ-NCPs (CD1)	75.6 %	82.4 %	85.3 %	85.3 %	88.8 %	88.8 %	93.4 %	93.4 %
CDZZ-NCPs (CD2)	78.5 %	86.9 %	86.9 %	88.3 %	89.0 %	91.2 %	93.0 %	93.4 %
CDZZ-NCPs (CD3)	81.3 %	87.9 %	89.7 %	90.8 %	93.0 %	93.4 %	97.8 %	98.5 %
CDZZ-NCPs (CD4)	91.3 %	92.8 %	93.9 %	95.8 %	97.7 %	97.7 %	98.1 %	99.0 %

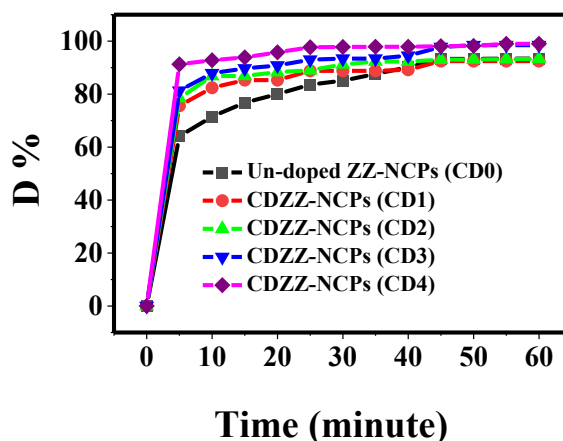


Fig. 6. Degradation rate, D% derived from fig 5 (b-f) with respect to the irradiation time.

nanocomposite is able to absorb and degrade the negative surface of CR anion. Therefore, nanocatalyst CDZZ-NCPs (CD0-4) is able to degrade the congo red dye easily. The degradation rate of un-doped/ CDZZ-NCPs (CD0-4) are presented in Table 4.

It is clear that the degradation rate of the CDZZ-NCPs (CD4) is higher than CDZZ-NCPs (CD0-3) [Fig. 5 (b-f)]. Notably, 91.3% of CR gets degraded after 5 minutes and 99.0% degradation happens after 60 minutes sunlight irradiation in the presence of the CDZZ-NCPs (CD4), while 64.1 %, 75.6 %, 78.5 % and 81.3 % has been reached after 5 minutes irradiation and 93.4 %, 93.4 %, 93.4 % and 98.5 % degradation happens after 60 minutes irradiation in the presence of the CDZZ-NCPs (CD0-3). It is obvious; the degradation rate is increasing with the increase of Cd-dopant concentration from CD0-4. This phenomenon is due to the presence of Cd-dopant in the electron layers. The presence of Cd in photocatalysts CDZZ-NCPs (CD1-4) causes a delay of the electrons return from the CB (conductive-band) to the VB (valence-band) [24-42]. Therefore, CDZZ-NCPs (CD1-4) show the best photodegradation of CR. All red lines in Fig. 5 (b-f)

show the degradation of nano composites CDZZ-NCPs (CD0-4) in dark.

The as-synthesized photocatalyst consists of three active components, including zinc zirconate, zinc oxide and zirconium dioxide ($ZnZrO_3/ZnO/ZrO_2$). When sunlight, which included UV and Vis lights, is used as a source of radiation, three photocatalyst portions can degrade CR by two mechanisms: photosensitized oxidation mechanism and photocatalytic oxidation mechanism [43], which improves the ability of a photocatalyst.

Fig. 6. demonstrates the percentage of degradation (D %) of CR mixed with un-doped ZZ-NCPs (CD0) and CDZZ-NCPs (CD1-4) which is obtained from the Fig. 5 (b-f). It is clear that the degradation rate of the CDZZ-NCPs (CD4) in the first 5 minutes (91.3%) is higher than un-doped and CDZZ-NCPs (CD0-3). The degradation rate is increasing with the increase of Cd-dopant concentration from CDZZ-NCPs (CD1-4).

CONCLUSION

The photocatalyst un-doped and Cd-doped of $ZnZrO_3/ZnO/ZrO_2$ prepared by hydrothermal

method and exhibits high photocatalytic efficiency. The purpose of this research is to investigate the degradation of CR dye by un-doped and Cd-doped ZnZrO₃/ZnO/ZrO₂ nano composites (CDZZ-NCPs) under sunlight for the first time. Structures were characterized using FT-IR, XRD, FE-SEM, EDS techniques and the UV-Vis absorption spectra was used to demonstrate the photocatalytic degradation of congo red (CR). The photocatalysts CDZZ-NCPs (CD4) showed the excellent photocatalytic ability (pH =14) for degradation of CR under sunlight irradiation. In the presence of the CDZZ-NCPs (CD4), 91.3% of CR gets gradate after 5 minutes, and 99.0% degradation happened after 60 minutes sunlight irradiation, while 64.1 %, 75.6 %, 78.5 % and 81.3 % has been reached after 5 minutes irradiation and 93.4 %, 93.4 %, 93.4 % and 98.5 % degradation happened after 60 minutes sunlight irradiation in the presence of the CDZZ-NCPs (CD0-3). It is obvious; the degradation rate is increasing with the increase of Cd-dopant concentration from CD0-4 [Fig. 5 (b-f)].

ACKNOWLEDGMENTS

The authors acknowledge Dr. Reza Rooydell for helpful guidance.

DISCLOSURE STATEMENT

All authors declare that they have no conflict of interest in the publication of this manuscript.

REFERENCES

- [1] Afkhami A., Moosavi R., (2010), Adsorptive removal of Congo red, a carcinogenic textile dye, from aqueous solutions by maghemite nanoparticles. *J. Hazard. Mater.* 174: 398-403.
- [2] Takei T., Haramoto R., Dong Q., Kumada N., Yonesaki Y., Kinomura N., Mano T., Nishimoto S., Kameshima Y., Miyake M., (2011), Photocatalytic activities of various pentavalent bismuthates under visible light irradiation. *J. Solid State Chem.* 184: 2017-2022.
- [3] Tang P., Chen H., Cao F., Pan G., (2011), Magnetically recoverable and visible-light-driven nanocrystalline YFeO₃ photocatalysts. *Catal. Sci. Technol.* 1: 1145-1148.
- [4] Singh J., Uma S., (2009), Efficient photocatalytic degradation of organic compounds by ilmenite AgSbO₃ under visible and UV light irradiation. *J. Phys. Chem. C.* 113: 12483-12488.
- [5] Hatakeyama T., Takeda S., Ishikawa F., Ohmura A., Nakayama A., Yamada Y., Matsushita A., Yea J., (2010), Photocatalytic activities of Ba₂RBiO₆ (R = La, Ce, Nd, Sm, Eu, Gd, Dy) under visible light irradiation. *J. Ceram. Soc. Jpn.* 118: 91-95.
- [6] Kanhere P., Chen Zh., (2014), A Review on visible light active perovskite-based photocatalysts. *Molecules.* 19: 19995-20022.
- [7] Habibi M-H., Askari E., Habibi M., Zendehelel M., (2013), Novel nanostructure zinc zirconate, zinc oxide or zirconium oxide pastes coated on fluorine doped tin oxide thin film as photoelectrochemical working electrodes for dye-sensitized solar cell. *Spectrochim. Acta Part A: Molec. Biomol. Spec.* 104: 197-202.
- [8] Zhu X., Zhou J., Zhu J., Liu Li. Y., Al-Kassab.T., (2014), Structural characterization and optical properties of perovskite ZnZrO₃ nanoparticles. *J. Am. Ceram. Soc.* 97: 1987-1992.
- [9] Oda A. M., Kadhum S. H., Farhood A. S., alkadhum H. A., (2014), Degradation of Congo red Solution by Zinc Oxide/Silver Composite Preheated at Different Temperatures. *J. Thermodyn. Catal.* 5: 1.
- [10] Movahedi M., Mahjoub A. R., Janitabar-Darzi S., (2009), Facile synthesis and characterization of CdTiO₃ nanoparticles by Pechini sol-gel method. *J. Iran. Chem. Soc.* 6: 570-577.
- [11] Elmorsi T. M., Elsayed M. H., Bakr M. F., (2017), Na doped ZnO nanoparticles assisted photocatalytic degradation of congo red dye using solar light. *Am. J. Chem.* 7: 48-57.
- [12] Chen X., Wu Zh., Liu D., Gao Zh., (2017), Preparation of ZnO photocatalyst for the efficient and rapid photocatalytic degradation of Azo Dyes. *Nanoscale Res. Lett.* 12: 143-148.
- [13] White J., Smith W., (2013), A brief note on the temperature-dependent photocatalytic degradation of congo red using Zinc Oxide. *Am. J. Water Res.* 1: 66-69.
- [14] Karamipour A., Rasouli N., Movahedi M., Salavati H., (2016), A kinetic study on adsorption of congo red from aqueous solution by ZnOZnFe₂O₄- polypyrrole magnetic nanocomposite. *Phys. Chem. Res.* 4: 291-301.
- [15] Esther Leena Preethi M., Umasankari A., Rekha C. H., (2018), Preparation of nanostructured TiO₂-based photocatalyst by controlling the calcining temperature and Ph. *Int. J. Recent Sci.Res.* 9: 25269-25273.
- [16] Aghabeygi S., Sharifi Z., Molahasani N., (2017), Enhanced photocatalytic property of nano--ZrO₂-SnO₂ NPs for photodegradation of azo dye. *Digest J. Nanomater. Biostruc.* 12: 81- 89.
- [17] Sapawe N., (2015), Hybridization of zirconia, zinc and iron supported on HY zeolite 1 as solar-based catalyst for rapid decolorization of various dyes. *New J. Chem.* 39: 4526-4533.
- [18] Jalili Kh., Aghabeygi Sh., Mirza B., (2016), Sonosynthesis and characterization of TiO₂/ZrO₂ nanocomposite and photocatalytic degradation of congo red dye under UV light. *J. Appl.Chem. Res.*10: 123-133.
- [19] Wang Ch., Le Y., Cheng B., (2014), Fabrication of porous ZrO₂ hollow sphere a ditsadsorption performance to congo red in water. *Ceram. Int.* 40: 10847-10856.
- [20] Ouyang J., Zhao. Z., Suib S. L., Yang H., (2019), Degradation of congo red dye by a Fe₂O₃@CeO₂-ZrO₂/Palygorskite composite catalyst: Synergetic effects of Fe₂O₃. *J. Colloid & Interf. Sci.* 539: 135-145.
- [21] Rooydell R., Wang R-Ch., Brahma S., Ebrahimzadeh F., Liu Ch-Pu., (2015), Synthesis and characterization of bis(acetylacetonato κ-O, O') [zinc(II)/copper(II)] hybrid organic-inorganic complexes as solid metal organic precursors. *Dalton Trans.* 44: 7982-7990.
- [22] Thananattanachon T., (2016), Synthesis and characterization of a perovskite barium zirconate (BaZrO₃): An experiment for an advanced inorganic chemistry laboratory. *J. Chem. Educ.* 93: 1120-1123.
- [23] Jasim Uddin M., Islam M. A., Haque Sh. A., Hasan S.,

- Amin M. Sh. A., Rahman M. M., (2012), Preparation of nanostructured TiO₂-based photocatalyst by controlling the calcining temperature and pH. *Int. Nano Lett.* 2: 19-23.
- [24] Konstantinou I. K., Albanis T. A., (2004), TiO₂-assisted photocatalytic degradation of azo dyes in aqueous solution: Kinetic and mechanistic investigations: A review. *Appl. Catal. B.* 49: 1–14.
- [25] Ahmed S., Rasul M. G., Martens W., Brown R., Hashib M. A., (2011), Advances in heterogeneous photocatalytic degradation of phenols and dyes in wastewater: A Review. *Water Air Soil Pollut.* 215: 3–29.
- [26] Rajesh J.T., Praveen K.S., Ramchandra G. K., Raksh V.J., (2007), Photocatalytic degradation of dyes and organic contaminants in water using nanocrystalline anatase and rutile TiO₂. *Sci. Technol. Adv. Mat.* 8: 455-459.
- [27] Bickley R. I., Vishwanathan V., (1979), Photocatalytically induced fixation of molecular nitrogen by near UV radiation. *Nature.* 280: 306–308.
- [28] Zhao J., Yang X., (2003), Photocatalytic oxidation for indoor air purification: A literature review. *Build. Environ.* 38: 645–654.
- [29] Wang H., Wu Z., Zhao W., Guan B., (2007), Photocatalytic oxidation of nitrogen oxides using TiO₂ loading on woven glass fabric. *Chemosphere.* 66: 185–190.
- [30] Bhalla A. S., Guo R., Roy R., (2000), The perovskite structure—a review of its role in ceramic science and technology. *Mat. Res. Innov.* 4: 3–26.
- [31] Damjanovic D., (2001), Piezoelectric properties of perovskite ferroelectrics: unsolved problems and future research. *Ann. Chim. Sci. Mat.* 26: 99–106.
- [32] Nuraje N., Su K., (2013), Perovskite ferroelectric nanomaterials. *Nanoscale.* 5: 8752–8780.
- [33] Jia Q., Iwase A., Kudo A., (2014), BiVO₄-Ru/SrTiO₃: Rh composite Z-scheme photocatalyst for solar water splitting. *Chem. Sci.* 5: 1513–1519.
- [34] Sayama K., Mukasa K., Abe R., Abe Y., Arakawa H., (2001), Stoichiometric water splitting into H₂ and O₂ using a mixture of two different photocatalysts and an IO₃⁻/I⁻ shuttle redox mediator under visible light irradiation. *Chem. Commun.* 23: 2416–2417.
- [35] Zhang W. F., Tang J., Ye J., (2006), Photoluminescence and photocatalytic properties of SrSnO₃ perovskite. *Chem. Phys. Lett.* 418: 174–178.
- [36] Lin. W. H., Cheng C., Hu C. C., Teng H., (2006), NaTaO₃ photocatalysts of different crystalline structures for water splitting into H₂ and O₂. *Appl. Phys. Lett.* 89: 211904-211909.
- [37] Shi. J., Guo. L., (2012), ABO₃-based photocatalysts for water splitting. *Prog. Nat. Sci. Mat. Int.* 22: 592–615.
- [38] Wang. W.N., Soulis. J., Jeffrey Yang. Y., Biswas. P., (2014), Comparison of CO₂ photoreduction systems: A review. *Aerosol Air Qual. Res.* 14: 533–549.
- [39] Tang. J., Durrant. J.R., Klug. D.R., (2008), Mechanism of Photocatalytic Water Splitting in TiO₂. Reaction of Water with Photoholes, Importance of Charge Carrier Dynamics, and Evidence for Four-Hole Chemistry. *J. Am. Chem. Soc.* 130: 13885–13891.
- [40] Kudo. A., Miseki. Y., (2009), Heterogeneous photocatalyst materials for water splitting. *Chem. Soc. Rev.* 38: 253–278.
- [41] Houas. A., Lachheb. H., Ksibi. M., Elaloui. E., Guillard. C., Herrmann. J.-M., (2001), Photocatalytic degradation pathway of methylene blue in water. *Appl. Catal. B.* 31: 145–157.
- [42] Turchi. C.S., Ollis. D.F., (1990), Photocatalytic degradation of organic water contaminants: Mechanisms involving hydroxyl radical attack. *J. Catal.* 122: 178–192.
- [43] Konstantinou. I. K., Albanis. T. A., (2004), TiO₂-assisted photocatalytic degradation of azo dyes in aqueous solution: kinetic and mechanistic investigations A review. *Applied Catalysis B: Environmental.* 49: 1–14.